RSC Advances

ROYAL SOCIETY OF CHEMISTRY

www.rsc.org/advances

Graphical abstract

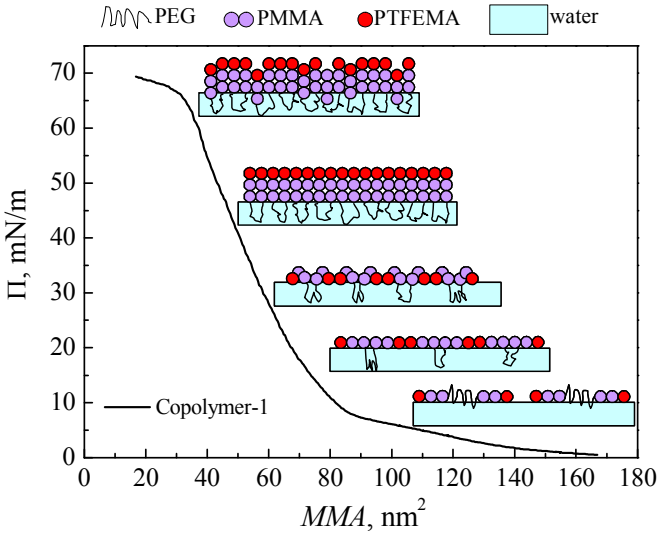

The interfacial rheology, aggregation behaviour and the packing model of structure evolution of three amphiphilic CBABC-type pentablock copolymers were investigated at the air-water interface.

Journal Name

ARTICLE

Interfacial rheology and aggregation behaviour of amphiphilic CBABC-type pentablock copolymers at the air-water interface: effects of block ratio and chain length

Received 00th January 20xx,
Accepted 00th January 20xx

DOI: 10.1039/x0xx00000x

www.rsc.org/

Zhiguang Li,[a b] Xiaoyan Ma,[*a b] Duyang Zang,[a c] Xinghua Guan,[a b] Lin Zhu,[a b] Jinshu Liu[a b] and Fang Chen[a b]

Interfacial rheology and aggregation behaviour of three amphiphilic CBABC-type pentablock copolymers possessing different block ratios and chain lengths were investigated at the air-water interface, in which C, B and A represent poly(trifluoroethyl methacrylate)/PTFEMA, poly(methyl methacrylate)/PMMA and poly(ethylene glycol)/PEG, respectively. The influence of block ratio and chain length on interfacial rheology of the Langmuir films was studied *via* continuous compression, successive addition and step compression methods. The surface pressure-mean molecular area isotherms and limiting mean molecular areas of the three copolymers were studied in the continuous compression. The surface pressure and modulus obtained from continuous compression and successive addition methods were compared. Furthermore, the relaxation of the monolayer was discussed by step compression method. The relaxation process was proposed that relating to the adsorption-desorption exchange of molecules and polymer segments on the surface (fast relaxation process) and reconformation of the adsorbed macromolecules inside the adsorption layer (slow relaxation process) at different mean molecular area of compression. In addition, the Langmuir-Blodgett (LB) films prepared at various surface pressures from the three copolymers were scanned by atom force microscopy (AFM) images, and a variety of morphologies such as macroporous, rugged, reticular and uncontinuous continent structures were observed. Finally, the packing model of structure evolution for the pentablock copolymers aggregate at the air-water interface was proposed.

1. Introduction

Amphiphilic block copolymers with complex architectures, different block ratios and chain lengths have attracted considerable attention due to their outstanding solution properties, such as their self-assembly in the presence of a selective solvent or surface.[1-3] In particular, The current interest in the properties of interfacial layers formed by this copolymers stems from their ability to spontaneously organize into ordered surface patterns.

Many amphiphilic copolymers tend to form an ordered monolayer with precise thickness and organized molecular assembly with well-defined molecular orientation when spread them at the air-water interface.[4-8] The surface morphologies of the monolayer can be easily adjusted by a lot of controllable factors, including chemical structure of copolymers as well as relative length of each block, surface pressure, molecular weight, and so on.[1, 7, 9-12] Through Langmuir film balance, we can obtain information about not only the mechanical properties and the interaction of molecules, but also the size, shape and the orientation of molecules.[7, 13] Duran *et al.* and Moffitt's group found that the surface morphologies of the copolymer depended on the relative amounts of hydrophobic and hydrophilic blocks of polystyrene-*b*-poly(ethylene oxide) (PS-*b*-PEO) in both linear and star systems.[14-17] The ability of the PS to aggregate into the surface morphologies was impacted by the ability of PEO to separate the PS chains, and these tendencies directly related to the block ratio and chain length.[18] Furthermore, Logan and co-workers[5] investigated the influence of PS on the morphologies of the monolayers by examining a series of PS-*b*-PEO containing constant PEO and variable chain lengths of PS, and found that the different morphologies of these copolymers formed were the nanostructures of exclusively dots, spaghetti and continents. In addition, the surface pressure at which a film was transferred led to apparent changes of aggregation in star PS-*b*-PEO systems.

The surface properties of the amphiphilic block copolymers have been widely studied by the Langmuir trough technique which allows the control of the nanostructures formed at the air-water interface.[19-23] The two-dimensional properties of the aggregates and the conformational changes of the copolymer chains induced by compression of the film can be derived from interfacial rheology.[24-27] Interfacial rheology of Langmuir fil

[a] *Key Laboratory of Space Applied Physics and Chemistry, Ministry of Education, Shaanxi province, School of Science, Northwestern Polytechnical University, Xi'an 710129, China.*
[b] *Key Laboratory of Polymer Science and Technology, Shaanxi province, School of Science, Northwestern Polytechnical University, Xi'an 710129, China.*
[c] *NPU-UM II Joint Lab of Soft Matter, School of Science, Northwestern Polytechnical University, Xi'an 710129, China*

† Electronic Supplementary Information (ESI) available: [Π-*MMA* isotherms of copolymer-3 with spreading amount of 0.025mg and BAM images of monolayer of copolymer-1 at collapse region (*MMA*=33.0nm^2)]. See DOI: 10.1039/x0xx00000x

is determined by a number of parameters, such as spreading concentration, compression rate, block ratio and chain length.[16, 17, 28-33] Furthermore, the investigation of interfacial rheology is used for understanding the viscoelastic properties,[34] which provides the modulus and relaxation behaviour.[35] Langevin *et al.*[36] investigated the compression modulus of acrylic Langmuir films, which related to the elastic energy stored by the surface layer upon compression. Relaxation reveals a nonequilibrium *via* step compression, and could obtain the dilational modulus. Our group[6] revealed the relaxation behaviour of the polystyrene-*b*-poly(acrylic acid) (PS-*b*-PAA) block copolymer. The modulus and two relaxation times of the monolayer were obtained from the fit of the relaxation isotherms. In particular, two types of relaxation mechanisms were involved from the two relaxation times, one was the exchange of molecules between the polymer solution and the interface, the other was the conformational change of molecules in the interfacial layer.[37]

In recent years, numerous investigations have been carried out on poly(ethylene glycol) (PEG) based block copolymers at the air-water interface.[4, 5, 38-41] The surface-active nature of PEG promotes its spontaneous adsorption at the air-water interface and causes it to become more easily dissolved in the aqueous subphase. The hydrophobic block of poly(trifluoroethyl methacrylate) (PTFEMA) with the advantage of hydrophobicity, low surface energy and good stability is the best candidate to tether PEG to the surface. To our knowledge, very little report has been put into fundamentally understanding the interfacial rheology and aggregation behaviour of PTFEMA based block copolymers at the air-water interface. Therefore, fundamental studies of PTFEMA based block copolymers performed at the interface can provide valuable interfacial phase behaviour in order to further guide their applications. In addition, the equilibrium behaviour of the PMMA based block copolymer films had been studied extensively in the decades.[2, 42-48] And for all we know, most of the investigations carried out at the air-water interface have paid more attention on AB-type diblock copolymers, while only a few studies had examined the aggregation of ABA-type multiblock copolymers,[4, 7, 49] and the multiblock copolymers treatment to adequately predict the aggregation and the interfacial rheology are still missing.

In order to reveal the self-assembly of PTFEMA based multiblock copolymers at the air-water interface, the interfacial rheology and aggregation behaviour of three amphiphilic CBABC-type pentablock copolymers of PTFEMA-*b*-PMMA-*b*-PEG-*b*-PMMA-*b*-PTFEMA with different block ratios and chain lengths are investigated. The aim of this study is to determine the precise influence of block ratio and chain length on the interfacial rheology. The isotherms of surface pressure and modulus in compression and successive addition methods are compared. The relaxation times and dilational modulus are discussed in the relaxation through step compression methods. Moreover, the morphologies of LB films prepared from the three copolymers at various surface pressures are also characterized. Finally, the packing model of the pentablock copolymers aggregate at the air-water interface is proposed.

2. Experimental

2.1. Materials

Three pentablock copolymers of PTFEMA-*b*-PMMA-*b*-PEG_{2000}-*b*-PMMA-*b*-PTFEMA with different molecular weights were synthesized *via* atom transfer radical polymerization in our previous study.[50] Gel permeation chromatography (GPC) analysis results were listed in Table 1. Water used in all experiments was de-ionized and ultrafiltrated to 18.2MΩ with an ELGA Lab water system. Chloroform ($CHCl_3$) was analytical pure and used without further purification. The spreading concentrations were prepared by weighting an appropriate amount of the copolymer into new glass reagent vials cleaned three times with acetone in an ultrasonic clean tank, and then a certain amount of $CHCl_3$ was added gravimetrically; all the solutions were prepared 6h prior to allow for equilibration.

2.2. Langmuir trough, isotherms of Langmuir films, BAM and AFM images

Isotherm characterization was accomplished using a Teflon Langmuir trough system (*W*=200mm, *L*=310mm, JML04C3, Powereach Ltd., China) equipped with two moving barriers and a Wilhelmy plate. The isotherms were measured with symmetric compression at a rate of 5mm/min at 20±2°C.

Three pentablock copolymers were spread at the air-water interface. In these experiments, the concentration of the solution was 0.3mg/mL, and the total mass of the copolymers were kept constant (0.015mg).

To prepare a Langmuir film (normally insoluble molecular films at the air-water interface), the three pentablock copolymers dissolved in $CHCl_3$ were spread dropwise on an ultral-pure water subphase using microsyringe, and the solvent was allowed to evaporate completely for 30 min. The surface concentrations were varied either by compressing the barriers or by adding small aliquots solution to the interface (successive addition).[36, 51, 52] Each small aliquot solution was spread in successive addition and evaporated for 5min. The relaxation was studied *via* step compression that the surface film was firstly compressed and afterwards the barriers were stopped to allow the relaxation of the monolayer. The relaxation curve was accepted only if the initial and final values of surface pressure were in agreement with the corresponding equilibrium values.[53]

The Langmuir trough was also equipped with a Brewster Angle Microscope (JB04, Powereach Ltd., China) to image the copolymer and its solution films at the interface.

Table 1. GPC analysis results of the pentablock copolymers

Serial Number	Block ratio PEG:PMMA:PTFEMA	M_n, g/mol	PDI
copolymer-1	9:21:15	26790	1.49
copolymer-2	9:21:11	23340	1.58
copolymer-3	9:11:7	17200	1.57

The LB films of the copolymers were the deposited films transferred onto glass substrate at various surface pressures. The glass substrate was immerged into water subphase before spreading copolymer solution. Following maintenance at target transfer pressure, the submerged substrate was lifted vertically through the film at a speed of 3mm/min. These transferred films were dried in vacuum desiccator for 24h at room temperature. The transferred LB films were scanned in tapping mode with AFM (MFP-3D-SA, Asylum Research Inc., USA) using silicon probes (AMCL-AC240, Olympus, Japan).

3. Results and discussion

3.1. Surface pressure-mean molecular area isotherms

Surface pressure (Π)-mean molecular area (*MMA*) isotherms of Langmuir films obtained from the compression of the three pentablock copolymers are depicted in Fig. 1. It is found that copolymer-1 and copolymer-2 exhibit four regions (pancake, pancake to brush transition, brush and collapse), which is similar to the results in previous researches.[6, 54] On the other hand, Π-*MMA* isotherm of copolymer-3 shows only three regions, lacking collapse region.

In the pancake region (Region A), macromolecules of the copolymer occupy a large mean molecular area on the water surface and do not contact with each other.[55] The compression causes only an increase in polymer density, resulting in surface pressure closing to zero.[6] In this case, the PEG chains are progressively dissolved in the aqueous subphase. In Region B, lateral compression may cause macromolecules to contact with each other and lead to the surface pressure rise slowly, implying the interaction exists between the macromolecules of the copolymer on the water surface. The smooth PEG chains begin to stretch and mostly loop into water, and the compression causes the extrusion of the PMMA chains.

Upon further compression till brush region (Region C), the PTFEMA chains are strongly compressed that surface pressure steeply increases, which implies that a larger enhancement of the interaction may be occurred.[55] At the end of Π-*MMA* isotherms (Region D) for copolymer-1 and copolymer-2, the surface pressure exhibits a tendency to level off. It indicates the monolayer may collapse owing to the over-compression of the copolymers and the formation of multilayer structures on the water surface.[6, 7] On the other hand, the surface pressure of copolymer-3 does not reach to collapse region and shows an increasing tendency in the end.

It is observed that the block ratio and hydrophobic chain length have a major impact on the profile of the isotherms, and with the increase of the hydrophobic/hydrophilic ratio and hydrophobic chain length, the transition of the monolayer would occur first.[3, 5] It is noteworthy that copolymer-1 has the longest hydrophobic chain length, which has the best effect on the phase transition and surface pressure. It causes the extrusion of hydrophobic chains which are relatively uncompressible at the end of the compression. On the other hand, copolymer-3 dose not reach to collapse region, which may be due to it has the lowest hydrophobic/hydrophilic ratio of the three copolymers. It could reach to the collapse point when spread more amount of it as shown in Fig. S1. Therefore, copolymer-3 retards the interaction of the molecules in the maximum packing density.

The limiting mean molecular areas of the pancake and brush conformations ($A_{0,p}$ and $A_{0,b}$, respectively) could be quantified by extrapolating tangents to the inflection points of the Π–*MMA* isotherms to a surface pressure of zero (Fig. 1). For the three copolymers, $A_{0,p}$ and $A_{0,b}$ are illustrated in Fig. 2.

As observed in Fig. 2, both the $A_{0,p}$, and $A_{0,b}$ of copolymer-1 are the highest, while $A_{0,p}$, and $A_{0,b}$ of copolymer-3 are the lowest. The values of $A_{0,p}$ and $A_{0,b}$ could be affected greatly by chain length of the copolymers. Copolymer-1 with the longest chain length occupies relatively the largest surface area, hence $A_{0,p}$ of copolymer-1 is the highest. In the brush region, the PEG chains are fully desorbed into water, therefore $A_{0,b}$ is mainly determined by both the chain lengths of PMMA and PTFEMA chains and the uncompressible interspaces between them. As a result, the $A_{0,b}$ of copolymer-1 is also the highest.

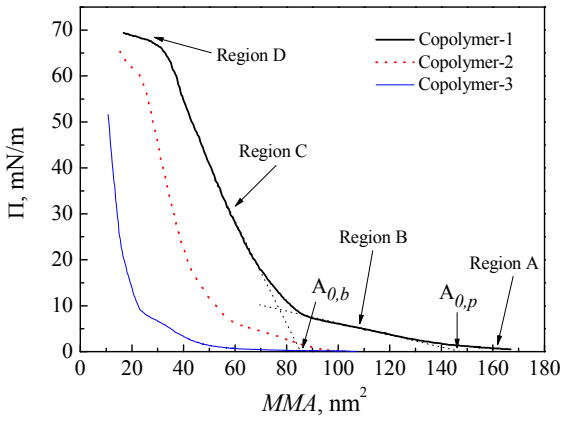

Fig. 1 Π-*MMA* isotherms of the three pentablock copolymers at the air-water interface upon compression. Determination of the brush and pancake limiting area $A_{0,b}$, $A_{0,p}$.

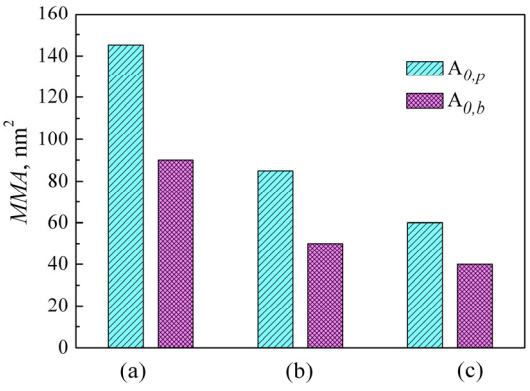

Fig. 2 Plots of pancake and brush limiting area $A_{0,p}$ and $A_{0,b}$ of copolymers determined from Π–*MMA* isotherms. (a) copolymer-1, (b) copolymer-2, (3) copolymer-3.

3.2. Interfacial rheology

It is convenient to derive the compression modulus (E) to investigate the interfacial rheology. The compression modulus gives information about the compactness and packing of the film,[56] which accounts for the elastic energy storage on the film upon compression.[2, 57] The compression modulus can be calculated from the derivative of the equilibrium surface pressure with respect to the surface concentration of copolymer Γ (The Π-Γ isotherms of the copolymers upon compression are exhibited in Fig. 3(a) come from Fig. 1),as the eqn (1):[58]

$$E = \Gamma\left(\partial\Pi/\partial\Gamma\right) \quad (1)$$

The E-Γ isotherms of the three copolymers are plotted in Fig. 3(b). It is found that the compression modulus may be correlated with the slope of the Π-Γ isotherm. Further compression is accompanied by an increase in E.[59] High E is a sign that the macromolecules are packed tightly and low interfacial fluidity among the packed molecules in Langmuir films. A monolayer with a high E value is rigid and difficult to deform. [56] Moreover, the peak value of E represents that the molecules are in the most compact arrangement and surface pressure increases rapidly.[33] The E is decreased for copolymer-1 and copolymer-2 afterwards, which is attributed to small value of dΠ/dΓ at higher pressure,[59] indicating that no more elastic storage is possible now.[60] Finally compression of the monolayer beyond the inflection point resulted in a collapse which manifested a steep decrease of the modulus. At the end of the collapse region the modulus decreases to a low level as consequence of the strong reduction of the available free area at the air-water interface and of the conformational freedom degrees of polymer chains.[61, 62] In this region relatively rigid monolayer fractured along straight strips. The strips piled up and formed multilayered structure as can be seen in the BAM image of copolymer-1 at collapse region (MMA=33.0nm^2). The BAM image is shown in Fig. S2 in the Supporting Information.

To further investigate the equilibrium and dynamic properties of the compression, the Π-Γ and E-Γ isotherms of successive addition are shown in Fig. 4(a) and (b), respectively. When a solution droplet is deposited on water surface, the PEG adsorbs at the interface and the hydrophobic blocks, that is strongly incompatible with PEG and water, tends to be segregated toward the air. Subsequently, as the solvent evaporates, the copolymer "pancake" spread over larger area. With the successive addition, the molecules gradually become closer, the mobility of the blocks becomes restricted because of both space limitations and the mutual interactions. In the same surface concentration, the surface pressure of copolymer-1 is also the highest in Fig. 4(a).

It is obvious that the modulus for the three copolymers exhibit a maximum value. In general, the successive addition has two aspects of influence on the surface modulus: one is to increase the surface concentration of copolymer and the other is

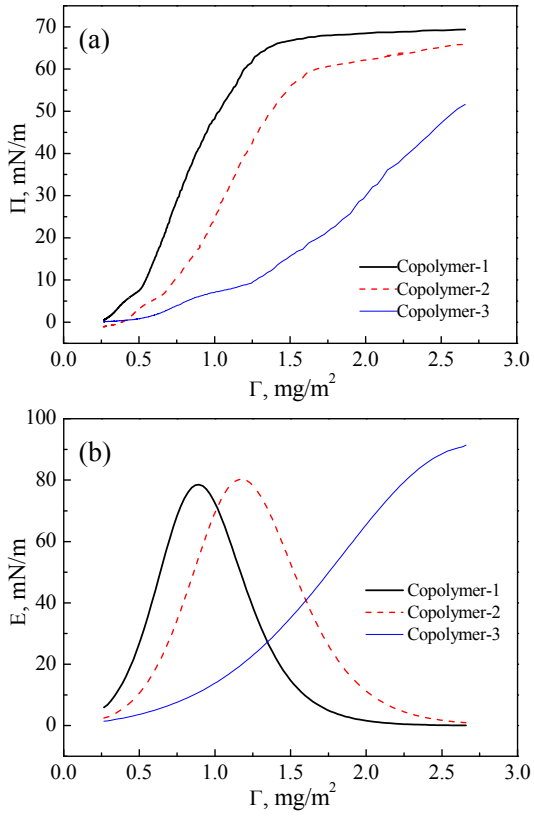

Fig. 3 Compression properties of the three pentablock copolymers. (a) Π-Γ isotherms. (b) E-Γ isotherms.

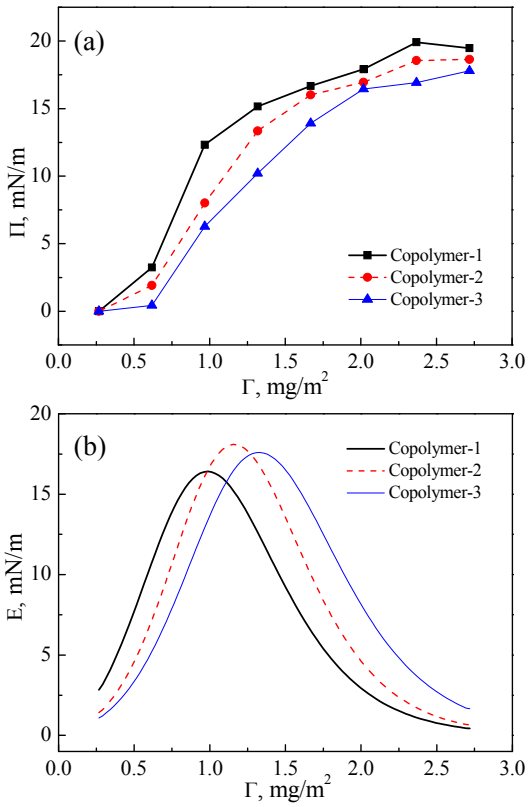

Fig. 4 Equilibrium properties of the three pentablock copolymers obtained from successive addition. (a) Π-Γ isotherms (b) E-Γ isotherms.

to increase the ability of copolymer molecules to diffuse from the bulk to the surface. The former can raise the surface pressure gradients, resulting in an increase in the modulus, and the latter may exert a contrary effect. When the concentration is low, the increase of concentration mainly affects the surface adsorption; therefore, the modulus increases with the surface concentration. With further increase of the surface concentration, the transfer of copolymer molecules from bulk to the air-water interface states to dominate, which leads to the decrease of modulus.[63]

From Fig.3 and Fig.4, It is found that the surface pressure and modulus in the successive addition are much lower than that of the compression.[19, 51, 52] Rubio *et al.*[53] had carried out continuous compression experiments and found that once the monolayer is in the semidilute regime, the copolymer monolayer was brought into nonequilibrium states. It is more probable that the continuous compression brings the system out of equilibrium, while the successive addition method reaches to equilibrium states and leads to the free arrangement of the molecules. The copolymer chains are weekly interacting, thus leading to lower values of surface pressure and modulus. It reveals weak interaction between the molecules, thereby leading to the low stability of the films.[64] Compared with the successive addition, the continuous compression indicates the formation of a critical concentrated solid state.

It has been reported that, the surface relaxation can provide a deep insight into the composition and structure of adsorbed layers which is related to the aggregation or repulsion of copolymer chains and conformational rearrangement of molecules.[6, 31, 65] Measuring the relaxation at the air-water interface through step compression is a very useful dynamics technique to characterize the viscoelasticity of the Langmuir films.[6, 52, 66] Fig. 5(a) shows the Π-t data of the relaxation behaviour of copolymer-1, and the variation of Π-*MMA* is shown in the inset of Fig. 5(a). It is found that the Π increases quickly and undergoes a sudden drop within a few seconds before tending to a new equilibrium value, illustrating that the continuous compression leads to nonequilibrium states.[19] This creates internal stress that acts as restoring force for recovering the initial state when strain ceases. As a consequence, a surface pressure gradient appears and then relaxes to its equilibrium value.[57] The macromolecular orientation and rearrangement in the higher surface pressure lead to stronger internal stress, which result in longer relaxation time.

As described in detail by Tschoegl,[67] the theory of linear viscoelasticity suggests that the △Π(t) relaxation transients can be described in terms of the sum of two decaying exponents and a plateau:

$$\triangle\Pi(t) = A_1 e^{-t/\tau_1} + A_2 e^{-t/\tau_2} + \triangle\Pi_\infty \qquad (2)$$

where △Π(t) is the value of △Π at any moment (t), τ_1 and τ_2 are relaxation times for fast and slow processes, which take part in the total relaxation process; A_1 and A_2 are constants which reflect the contribution of the fast and slow relaxation times, respectively, to the total relaxation process, and $\triangle\Pi_\infty$ is the equilibrium value of △Π reached at the end of the relaxation.

To further study the microscopic relaxation process and the relaxation mechanism based on the analysis above, we used a exponential function to fit Π *versus* t curve obtained in the relaxation experiment. In the simplest case, when there is only one relaxation time, the pressure varies exponentially with time as $e^{-t/\tau}$ (τ is the relaxation time).[6, 65] Here we choose single exponential and two exponentials to fit the relaxation curves.

The time variation of surface dilational modulus can be obtained as eqn (3) and (4):

$$E(t) = E_0 e^{-t/\tau} + \triangle E_\infty \qquad (3)$$

$$E(t) = E_1 e^{-t/\tau_1} + E_2 e^{-t/\tau_2} + \triangle E_\infty \qquad (4)$$

where E is the surface modulus; E_0, E_1 and E_2 are the moduli corresponding to different relaxation times τ, τ_1 and τ_2, and $\triangle E_\infty$ is the equilibrium value at the end of the relaxation.

As depicted in Fig. 5(b), we found that the two exponential fitting curves fit the second and third relaxation curves better than the single exponential one. However, the first relaxation curve is better for the single exponential one. The main interest of the fits is to obtain the dilational moduli and relaxation times of the copolymer films. The dilational modulus at short time can be obtained as $E(0)=E_1+E_2$. The values of the dilational moduli and the relaxation times deduced from fits of Π–t evolution with eqn (3) and (4) are listed in Table 2.

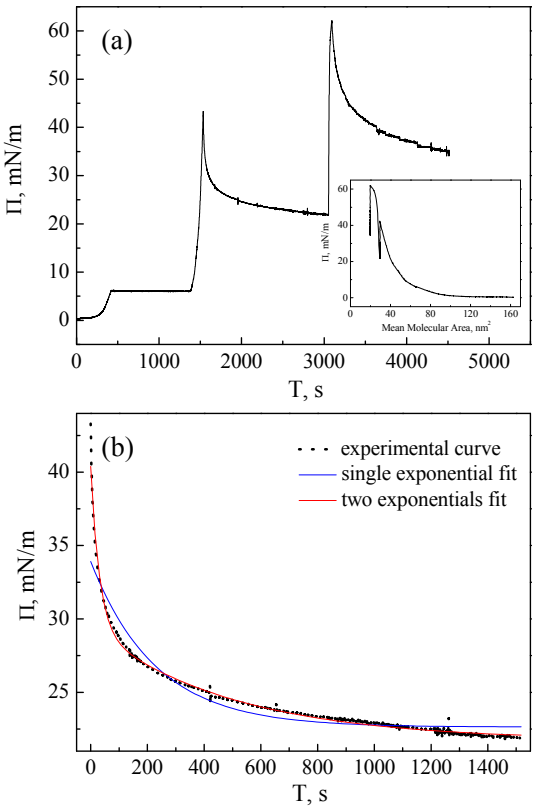

Fig. 5 (a) Surface pressure as a function of time in a step compression of copolymer-1. The inset corresponds to step compression Π-*MMA* isotherms of (a). (b) Examples of relaxation curve and the corresponding two fitting curves at the *MMA* of 53nm^2 of copolymer-1.

Table 2. Surface dilational moduli and the relaxation times from fits of Π-t evolution with eqn (3) and (4)

copolymers	*MMA*, nm^2	E_1, mN/m	τ_1, s	E_2, mN/m	τ_2, s	F_1 (%)	F_2 (%)	$E(0)$, mN/m	E, mN/m
	108	0.12	163.90	—	—	—	—	0.12	16.04
copolymer-1	53	10.98	30.45	7.67	496.33	8.07	91.93	18.65	76.12
	36	11.86	58.07	15.50	594.30	6.96	93.04	27.36	44.18
	69	0.35	145.96	—	—	—	—	0.35	15.37
copolymer-2	33	8.88	23.68	5.78	348.59	9.45	90.55	14.66	80.23
	26	13.53	82.12	16.30	1807.89	3.63	96.37	29.83	52.86
	37	0.58	131.38	—	—	—	—	0.58	8.11
copolymer-3	18	7.54	20.41	5.51	338.70	7.62	92.38	13.05	39.16
	13	10.92	58.80	13.93	540.83	7.85	92.15	24.85	75.66

As evidenced in Table 2, the times necessary for surface pressure to reach constant value are all quite long in different regimes. The relaxation time increased with the decreasing *MMA*. The good fit of second and third relaxation curves using eqn (4) suggests that there are two physical mechanisms dominate the relaxation including fast and slow processes.[68, 69]

The fractional contributions of the fast (F_1) and slow (F_2) relaxation processes can be obtained as eqn (5) and (6):[70]

$$F_1 = \frac{E_1\tau_1}{E_1\tau_1 + E_2\tau_2} \times 100 \quad (5)$$

$$F_2 = \frac{E_2\tau_2}{E_1\tau_1 + E_2\tau_2} \times 100 \quad (6)$$

It is closely acquainted with the fast relaxation process with a characteristic time values (fast relaxation time τ_1) in several tens of seconds involving adsorption-desorption exchange of molecules and polymer segments on the surface.[38] On the other hand, the slow relaxation process with a characteristic relaxation time values (slow relaxation time τ_2) from several hundreds to thousands of seconds, depending on slower reconformations of the adsorbed macromolecules inside the adsorption layer.[38] It is manifested that the smaller the mean molecular area is, the longer the fast and slow relaxation times are in Table 2.

In the first relaxation curve, there is only one relaxation process which can be regard as the fast relaxation process dominating the dynamic properties. It is believed to be related to the adsorption-desorption exchange of the hydrophilic chains on water surface. The PEG chains are located at the air-water interface flatly before compression. With the compression, the PEG chains adsorb on the water surface may be attributed to the rearrangement of the molecules. In the second and third relaxation curve, both the fast and slow relaxation processes influence the relaxation, and it is found that the slow relaxation dominates the global process in Table 2.

The relaxation times are also dependent on the molecular weight and molecular architecture. In particular, copolymer-3 possesses the shortest relaxation times τ_1 and τ_2, which indicates the fastest adsorption-desorption exchange and a rapid molecular reorganization of the copolymer chains adsorbed at the interface probably as a result of the lowest hydrophobicity and molecular weight.[38]

In the same mean molecular area, the compression modulus E and dilational modulus $E(0)$ are compared as observed in Table 2. It is found that compression modulus is higher than dilational modulus. The continuous compression is a nonequilibrium and dynamics process, and the molecules do not have time to relax. Therefore, the molecules in the compression aggregate denser than in the relaxation process, and the modulus is higher in the continuous compression than that of in the step compression.

3.3. Surface morphologies of LB films

To highlight the block ratio, chain length and surface pressure dependence of surface morphologies, the monolayer was transferred to glass substrate from water subphase. The submerged substrate was lifted vertically to air, resulting in the film containing hydrophobic chains sitting on top. Therefore, the brighter domains represent hydrophobic chains while the darker background reflects PEG or bare glass.[5, 6] Representative AFM images are shown in Fig. 6 and 7.

As depicted in Fig. 6, the typical features are observed for the three copolymers at 30mN/m on the isotherms. For copolymer-1, the images in Fig. 6(a) exhibit light raised rings surrounded by darker irregular rodlike aggregates. For copolymer-2 as depicted in Fig. 6(b), the morphology is a macroporous structure with black irregular holes. As observed in Fig. 6(c) for copolymer-3, the morphology is a rugged structure with uncontinuous continent, darker irregular aggregates. The LB films show very large empty spaces between the domains as the chain length decreased. Both the size and the shape of the domains seem to strongly depend on the molecular weight, block ratio and chain length,[4, 5] which is influenced by the chemical structure of the copolymer.

The importance of PEG, PMMA and PTFEMA composition helps explain the nanostructures seen through AFM images. The PEG chains are progressively dissolved in the water subphase. As a result, the morphologies of the LB films are determined by the PTFEMA and PMMA chains. A denser continent monolayer is found in Fig. 6(a) due to the largest hydrophobic ratio and chain length of copolymer-1. The most prevalent hydrophobic block of this copolymer could thus directly produce a less extended film structure that contains the largest aggregates. With the decrease of hydrophobic block ratio and chain length, the continuous region disappears and uncontinuous continents appear (Fig. 6(b) and (c)).

In addition, the influence of surface pressure on the assembly of the pentablock copolymer is also examined. Fig. 7 shows the typical AFM images of copolymer-2 at different surface pressures (5mN/m, 30mN/m and 62mN/m).

As exhibited in Fig. 7(a), there are a few bright spots widely separated at 5mN/m. The restructuring of the monolayer attributed to the initial spontaneous aggregation and conformation of PEG chains due to their submergence in the water subphase during compression.[1] The aggregations of dark regions among the hydrophobic chains are supposed to PEG chains. As the surface pressure increases to 30mN/m, a reticular structure is observed in Fig.7 (b). The film is compact, and more bright regions are appeared with the compression. The block chains are rearrange at the interface, and the motion of copolymer aggregates inside the film may result in the conformation change. When the surface pressure rises up to 62mN/m, the formation of densely packed structures is caused by lateral compression of the relatively uncompressible hydrophobic chains.

The roughness data of the three LB films of copolymer-2 are increased from 299.2, 419.6 to 974.1pm. From the 3D images and the roughness data, it is found that the roughness of the aggregation is increased by enhancing the surface pressure. This is interpreted as either the molecule is forced to alter its conformation due to the vicinity of its nearest neighbors with the increasing compression, or a densification of the packing of the copolymer molecules at a given surface pressure be derived from these LB depositions. The aggregates transformation change from relatively dispersive structures to continuous structures upon compression is due to the rebuilt of the hydrophobic chains by lateral compression.

From the results above, the changes in the morphologies obtained from different copolymers of the same surface pressure and different transferred regions of the identical copolymer are apparent. The block ratio and chain length of the copolymers and surface pressure play an important role in the morphologies of the LB films, and this is similar to the result in previous research by Deschênes *et al*.[4]

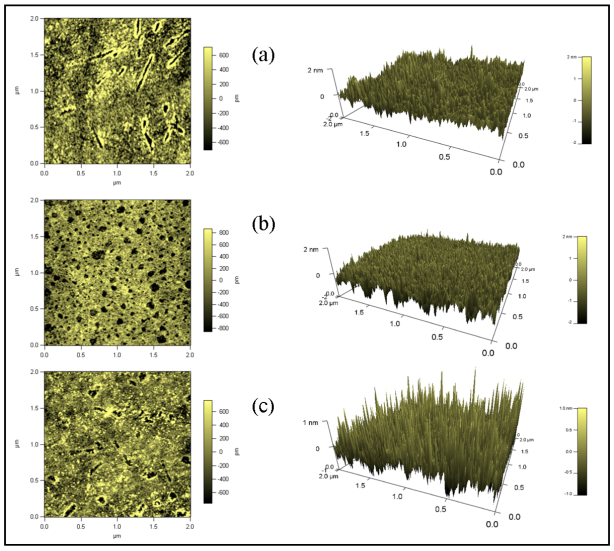

Fig. 6 Topography (left) and 3D (right) images of pentablock copolymer LB films transferred from brush region (30mN/m) on glass substrates: (a) copolymer-1, (b) copolymer-2, (c) copolymer-3.

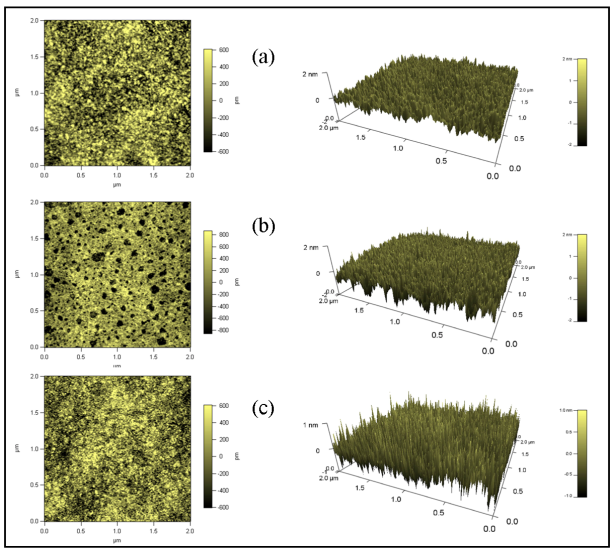

Fig. 7 Topography (left) and 3D (right) images of copolymer-2 LB fil transferred at different surface pressure on glass substrates: (a) 5mN/m, (b) 30mN/m, (c) 62mN/m.

3.4. Proposed packing model of the aggregation formation

From the analyses above, the packing model of the pentablock copolymers aggregate at the air-water interface is proposed i Fig. 8.

At Π≈0mN/m, the copolymers are spread completely with disordered dispersion and occupied a large surface area as depicted in Fig. 8(a). Lateral compression causes an increase in polymer density, and the orientation of the molecules may be occurred as shown in Fig. 8(b). In this case, the copolymer chains float on the water surface and adopt a flattened conformation on the water surface with maximum contacts with the water surface (pancake conformation). Upon furth compression, the copolymer molecules start to contact (Fig. 8(c)), the PEG chains are progressively dissolved in the water subphase; in this circumstances, the underneath hydrophobic groups, making surface pressure and compression modulus increase. As compression proceeds, compared the rigid of the PMMA and PTFEMA, the smooth PEG chains begin to stretch and mostly loop into water in Fig. 8(d). Further compression causes the extrusion of the PMMA chains as shown in Fig. 8(e). Parts of the PMMA chains detach on the water surface and aggregate into thicker domains, which represent a transition of the pancake to brush conformation of the monolayer. The chains are strongly interacted that the surface pressure rapidly increases. And then the hydrophobic groups prone to vertical as shown in Fig. 8(f) with compression, the hydrophobic chains are densely packed and kept in touch with each other. At this point, the monolayer completely covers the surface in a unifor phase and the copolymer molecules reorganize into a brush conformation. The last compression leads to the film collapse which is attributed to over-compression of relative y uncompressible hydrophobic chains (Fig. 8(g)),[7] and th compression modulus starts to decrease.

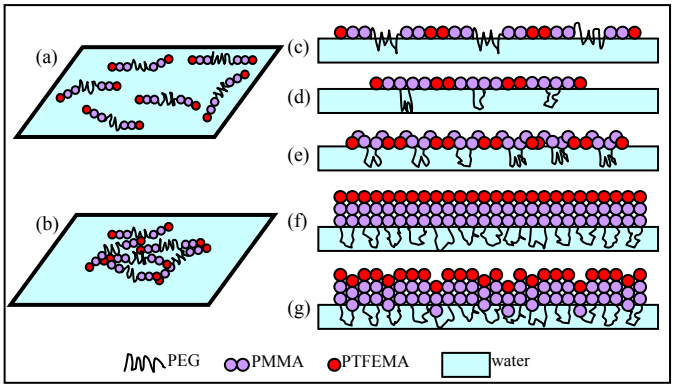

Fig. 8 Proposed packing model of structure evolution for the pentablock copolymers based on the isotherms and AFM images.

4. Conclusions

In this paper, the interfacial rheology and aggregation behaviour of the amphiphilic CBABC-type pentablock copolymers PTFEMA-*b*-PMMA-*b*-PEG-*b*-PMMA-*b*-PTFEMA with different block ratio and chain length are investigated at the air-water interface.

The influence of block ratio and chain length on interfacial rheology of the Langmuir films was studied *via* continuous compression, successive addition and step compression methods. It is found that copolymer-1 and copolymer-2 show four phase transition regions in the Π-*MMA* isotherms, while copolymer-3 lacks collapse region. The higher hydrophobic ratio and hydrophobic chain length are, the larger surface pressure in the same mean molecular area is, as well as the limiting mean molecular area. Compare to the successive addition, the higher values of surface pressure and modulus are observed in continuous compression due to strongly interacting of the chains.

In addition, the relaxation of the monolayer is investigated through step compression. It is found that there are two relaxation processes (fast and slow relaxation processes) in the second and third relaxation curves, while only one relaxation process in the first curve. The fast relaxation process attributed to adsorption-desorption exchange of molecules and polymer segments on the surface. Meanwhile, the slow relaxation process dominates by slower reconformations of the adsorbed macromolecules inside the adsorption layer. Furthermore, the LB films prepared at various surface pressures from the three copolymers have a variety of morphologies such as macroporous, rugged, reticular and uncontinuous continent structures result from the block ratio, chain length and surface pressure. Finally, the packing model of the pentablock copolymer aggregates at the air-water interface is proposed.

Acknowledgements

This work is supported by the National Natural Science Foundation of China (Grant no. 51372206, 51301139), Natural Science Foundation of Shaanxi Province (Grant no. 2013JM2012), Innovation Project of Science and Technology of Shaanxi Province (Grant no.2013KTCG01-14) and NPU Foundation for Fundamental Research (Grant no.3102014JCQ01089).

Notes and references

1 M. J. Felipe, N. Estillore, R. B. Pernites, T. Nguyen, R. Ponnapati and R. C. Advincula, *Langmuir*, 2011, **27**, 9327-9336.
2 A. Maestro, F. Ortega, F. Monroy, J. Krägel and R. Miller, *Langmuir*, 2009, **25**, 7393-7400.
3 T. J. Joncheray, K. M. Denoncourt, M. A. R. Meier, U. S. Schubert and R. S. Duran, *Langmuir*, 2007, **23**, 2423-2429.
4 L. Deschenes, M. Bousmina and A. M. Ritcey, *Langmuir*, 2008, **24**, 3699-3708.
5 C. P. Glagola, L. M. Miceli, M. A. Milchak, E. H. Halle and J. L. Logan, *Langmuir*, 2012, **28**, 5048-5058.
6 X. Wang, X. Ma and D. Zang, *Soft Matter*, 2013, **9**, 443-453.
7 W. Lee, S. Ni, J. Deng, B.-S. Kim, S. K. Satija, P. T. Mather and A. R. Esker, *Macromolecules*, 2007, **40**, 682-688.
8 J. Y. Park and R. C. Advincula, *Soft Matter*, 2011, **7**, 9829-9843.
9 I. I. Perepichka, A. Badia and C. G. Bazuin, *ACS Nano*, 2010, **4**, 6825-6835.
10 E. W. Price, S. Harirchian-Saei and M. G. Moffitt, *Langmuir*, 2010, **27**, 1364-1372.
11 S. Harirchian-Saei, M. C. P. Wang, B. D. Gates and M. G. Moffitt, *Langmuir*, 2010, **26**, 5998-6008.
12 I. I. Perepichka, K. Borozenko, A. Badia and C. G. Bazuin, *J. Am. Chem. Soc.*, 2011, **133**, 19702-19705.
13 L. Zhao, C. Feng, X. Pang, J. Jung, M. C. Stefan, P. Sista, R. Han, N. Fang and Z. Lin, *Soft Matter*, 2013, **9**, 8050-8056.
14 J. L. Logan, P. Masse, B. Dorvel, A. M. Skolnik, S. S. Sheiko, R. Francis, D. Taton, Y. Gnanou and R. S. Duran, *Langmuir*, 2005, **21**, 3424-3431.
15 J. L. Logan, P. Masse, Y. Gnanou, D. Taton and R. S. Duran, *Langmuir*, 2005, **21**, 7380-7389.
16 R. B. Cheyne and M. G. Moffitt, *Langmuir*, 2005, **21**, 5453-5460.
17 R. B. Cheyne and M. G. Moffitt, *Langmuir*, 2006, **22**, 8387-8396.
18 L. Zhao and Z. Lin, *Soft Matter*, 2011, **7**, 10520-10535.
19 H. Hilles, A. Maestro, F. Monroy, F. Ortega, R. G. Rubio and M. G. Velarde, *J. Chem. Phys.*, 2007, **126**, 124904.
20 A. Maestro, L. J. Bonales, H. Ritacco, T. M. Fischer, R. G. Rubio and F. Ortega, *Soft Matter*, 2011, **7**, 7761-7771.
21 D. Zang, A. Stocco, D. Langevin, B. Wei and B. P. Binks, *Phys. Chem. Chem. Phys.*, 2009, **11**, 9522-9529.
22 A. Maestro, E. Guzmán, E. Santini, F. Ravera, L. Liggieri, F. Ortega and R. G. Rubio, *Soft Matter*, 2012, **8**, 837-843.
23 C. Stefaniu, G. Brezesinski and H. Möhwald, *Sci Adv. Colloid Interface Sci.*, 2014, **208**, 197-213.
24 J. Maldonado-Valderrama, A. Martín-Rodriguez, M. J. Gálvez-Ruiz, R. Miller, D. Langevin and M. A. Cabrerizo-Vílchez, *Colloid. Surf. A: Physicochem. Eng. Asp.*, 2008, **323**, 116-122.
25 B. A. Noskov, G. Loglio and R. Miller, *Sci Adv. Colloid Interface Sci.*, 2011, **168**, 179-197.
26 B. A. Noskov, *Curr. Opin. Colloid Interface Sci.*, 2010, **15**, 229-236.
27 C. Kotsmar, V. Pradines, V. S. Alahverdjieva, E. V. Aksenenko, V. B. Fainerman, V. I. Kovalchuk, J. Krägel, M. E. Leser, B. A. Noskov and R. Miller, *Sci Adv. Colloia Interface Sci.*, 2009, **150**, 41-54.
28 J. Miñones, M. M. Conde, E. Yebra-Pimentel and J. M. Trillo, *J.Phys. Chem. C*, 2009, **113**, 17455-17463.

29 T. Morioka, O. Shibata and M. Kawaguchi, *Langmuir*, 2010, **26**, 18189-18193.
30 T. Morioka, O. Shibata and M. Kawaguchi, *Langmuir*, 2010, **26**, 14058-14063.
31 A. Maestro, H. M. Hilles, F. Ortega, R. G. Rubio, D. Langevin and F. Monroy, *Soft Matter*, 2010, **6**, 4407-4412.
32 K. N. Witte, S. Kewalramani, I. Kuzmenko, W. Sun, M. Fukuto and Y.Y. Won, *Macromolecules*, 2010, **43**, 2990-3003.
33 E. Spigone, G.-Y. Cho, G. G. Fuller and P. Cicuta, *Langmuir*, 2009, **25**, 7457-7464.
34 R. Miller, J. Ferri, A. Javadi, J. Krägel, N. Mucic and R. Wüstneck, *Colloid Polym. Sci.*, 2010, **288**, 937-950.
35 T. Naolou, K. Busse, B.-D. Lechner and J. Kressler, *Colloid Polym. Sci.*, 2014, **292**, 1199-1208.
36 L. R. Arriaga, F. Monroy and D. Langevin, *Soft Matter*, 2011, **7**, 7754-7760.
37 Y. Guo, T. Chen, N. Zhao, Y. Shang and H. Liu, *Colloid Polym. Sci.*, 2013, **291**, 845-854.
38 J. Juárez, S. Goy-López, A. Cambón, M. A. Valdez, P. Taboada and V. c. Mosquera, *J. Phys. Chem. C*, 2010, **114**, 15703-15712.
39 W. M. de Vos, A. de Keizer, J. M. Kleijn and M. A. Cohen Stuart, *Langmuir*, 2009, **25**, 4490-4497.
40 S. Vanslambrouck, B. Clement, R. Riva, L. H. Koole, D. G. M. Molin, G. Broze, P. Lecomte and C. Jerome, *RSC Adv.*, 2015, **5**, 27330-27337.
41 X. Wang, G. Wen, C. Huang, Z. Wang and Y. Shi, *RSC Adv.*, 2014, **4**, 49219-49227.
42 Y. Seo, C. Y. Cho, M. Hwangbo, H. J. Choi and S. M. Hong, *Langmuir*, 2008, **24**, 2381-2386.
43 B. Chung, H. Choi, H.W. Park, M. Ree, J. C. Jung, W. C. Zin and T. Chang, *Macromolecules*, 2008, **41**, 1760-1765.
44 Y. Sasaki, N. Aiba, H. Hashimoto and J. Kumaki, *Macromolecules*, 2010, **43**, 9077-9086.
45 N. Mitsui, T. Morioka and M. Kawaguchi, *Colloid. Surf. A-Physicochem. Eng. Asp.*, 2012, **395**, 248-254.
46 A. Maestro, F. Ortega, R. G. Rubio, M. A. Rubio, J. Krägel and R. Miller, *J. Chem. Phys.*, 2011, **134**, 104704.
47 Z. Wang, G. Wen, F. Zhao, C. Huang, X. Wang, T. Shi and H. Li, *RSC Advances*, 2014, **4**, 29595-29603.
48 G. Li Destri, F. Miano and G. Marletta, *Langmuir*, 2014, **30**, 3345-3353.
49 K. Busse, C. Peetla and J. Kressler, *Langmuir*, 2007, **23**, 6975-6982.
50 Z. Li, X. Ma, D. Zang, B. Shang, X. Qiang, Q. Hong and X. Guan, *RSC Adv.*, 2014, **4**, 49655-49662.
51 A. Stocco, E. Rio, B. P. Binks and D. Langevin, *Soft Matter*, 2011, **7**, 1260-1267.
52 D. Zang, E. Rio, D. Langevin, B. Wei and B. Binks, *Eur. Phys. J. E: Soft Matter Biol. Phys.*, 2010, **31**, 125-134.
53 H. M. Hilles, M. Sferrazza, F. Monroy, F. Ortega and R. G. Rubio, *J. Chem. Phys.*, 2006, **125**, 074706.
54 D. Langevin and F. Monroy, *Curr. Opin. Colloid Interface Sci.*, 2010, **15**, 283-293.
55 K. Kita-Tokarczyk, M. Junginger, S. Belegrinou and A. Taubert, in *Self Organized Nanostructures of Amphiphilic Block Copolymers II*, eds. A. H. E. Müller and O. Borisov, Springer Berlin Heidelberg, 2011, vol. 242, pp. 151-201.
56 B. Gzyl-Malcher, M. Filek and G. Brezesinski, *Langmuir*, 2011, **27**, 10886-10893.
57 F. Monroy, F. Ortega, R. G. Rubio and M. G. Velarde, *Sci Adv. Colloid Interface Sci.*, 2007, **134–135**, 175-189.
58 G. L. Gaines, *Insoluble monolayers at liquid-gas interfaces*, Interscience Publishers, New York, 1966.
59 N. Chaudhary and R. Nagaraj, *J. Colloid Interface Sci.*, 2011, **360**, 139-147.
60 F. Monroy, F. Ortega, R. G. Rubio, H. Ritacco and D. Langevin, *Phys. Rev. Lett.*, 2005, **95**, 056103.
61 H. M. Hilles, F. Ortega, R. G. Rubio and F. Monroy, *Phys. Rev. Lett.*, 2004, **92**, 255503.
62 B. Martín-García, M. M. Velázquez, J. A. Pérez-Hernández and J. Hernández-Toro, *Langmuir*, 2010, **26**, 14556-14562.
63 Y. J. Chen, T. Liu, G. Y. Xu, J. Zhang, X. R. Zhai, J. Yuan and Y. B. Tan, *Colloid Polym. Sci.*, 2015, **293**, 97-107.
64 H. Zhu, J. Matsui, S. Yamamoto, T. Miyashita and M. Mitsuishi, *Soft Matter*, 2015, **11**, 1962-1972.
65 F. Monroy, H. M. Hilles, F. Ortega and R. G. Rubio, *Phys. Rev. Lett.*, 2003, **91**, 268302.
66 G. A. Georgiev, N. Yokoi, S. Ivanova, V. Tonchev, Y. Nencheva and R. Krastev, *Soft Matter*, 2014, **10**, 5579-5588.
67 N. Tshoegl, Springer Verlag, Berlin, 1989, pp. 445-457.
68 D. Zang and Y. Zhang, *Sci. China-Phys. Mech. Astron.*, 2011, **54**, 1587-1592.
69 Y.Y. Wang, Y.H. Dai, L. Zhang, L. Luo, Y.P. Chu, S. Zhao, M.Z. Li, E.J. Wang and J.Y. Yu, *Macromolecules*, 2004, **37**, 2930-2937.
70 S. I. Lopes, A. M. Gonçalves da Silva, P. Brogueira, S. Piçarra and J. Martinho, *Langmuir*, 2007, 23, 9310-9319.